DEBOND DAMAGE ASSESSMENT IN FOAM / COMPOSITE SANDWICH STRUCTURES

R.K. Fruehmann[1], J.M. Dulieu-Barton[1]*, W. Wang[1]
[1] Faculty of Engineering and the Environment, University of Southampton, Southampton, UK
*(janice@soton.ac.uk)

Keywords: *Thermoelastic stress analysis, non-destructive testing, damage, sandwich structures*

1 Introduction

Debonds can occur sandwich structures for a wide variety of reasons, at the manufacturing stage as well as during the service life of the structure. The presence of such defects will serve to reduce the ultimate strength and stiffness of the structure, especially in bending, and may lead to catastrophic failure below the design loads. In evaluating the serviceability of a structure that contains a debond, it is important to understand how the stresses are redistributed around the defective region, and how easily a crack will propagate from this region. In this work, thermoelastic stress analysis (TSA) is used to study the stress field in both the face sheet and the foam core of a composite sandwich structure with a simulated debond between the face sheet and the core. Since this type of damage is often not visible on the surface of the material, locating and assessing the severity of face sheet / core debonds poses a significant challenge for the inspection of composite sandwich structures [1].

The present paper describes the use of infrared thermography to address three challenges and therefore permit an enhanced understanding of the nature of debond growth. The first is associated with the identification of the debonded region, not only in terms of locating it spatially but also with regard to a qualitative assessment of the extent of the debond. Secondly a first attempt is made to relate the heating at the edge of the debond with the fracture energy associated with the growth of the debond. Thirdly, an evaluation of the stresses through the thickness of the core near the crack tip region is required to better understand how the failure initiates.

2 Background to TSA

TSA was selected as the tool to evaluate the debonds because it is a full-field non-contacting technique. Therefore, there is no chance of reinforcing the sandwich polymer foam core. Moreover very high resolution data can be obtained by means of an infra-red detector directly from the vicinity of the interface defect. TSA is based on the measurement of small changes in surface temperature that can be related to changes in the sum of the principal stresses for an orthotropic material [2]:

$$\Delta T/T = \left(-1/\rho C_p\right)\Delta(\alpha_1\sigma_1 + \alpha_2\sigma_2) \quad (1)$$

where ΔT is the temperature change, T is the absolute temperature, α_1 and α_2 are the coefficients of thermal expansion, ρ is the density, C_p is the specific heat at constant pressure and $\Delta(\sigma_1 + \sigma_2)$ is the change in the sum of the principal stresses.

3 Experimental Arrangements

Sandwich panels were manufactured in a single shot resin infusion process using a closed cell PVC foam core (DIAB H100) and E-glass / epoxy composite face sheets. The composite face sheet comprised 8 plies of 210 gm^{-2} E-glass textile with a 1.1 mm and 1.7 mm yarn spacing in the warp and weft directions respectively. The woven composite used in the face sheets has been shown to have a *quasi*-isotropic homogenous thermoelastic response at the macro-scale, despite the orthogonal and heterogeneous nature of the individual yarns making the weave [3]. It is therefore possible to assume the isotropic form of equation (1) when assessing the distribution of stresses across the specimen surface.

Two types of test arrangement were used: a four point bend test and a double cantilever beam (DCB) test.

For the specimens used in the four point bend test a thin polytetrafluoro ethylene (PTFE) non-stick polymer film was placed between the glass fibres and the core prior to introducing the resin to create a controlled debond region. Beams were then cut from

the panel, 400 mm long by 50 mm wide, with the seeded debond located in the centre of the beam and spanning its full width. The samples in this work had a film thickness of 40 μm. The results from three different lengths of defect are presented in this work: 6, 12 and 18 mm. One set of beams was also made without the seeded damage for reference.

The four point bend rig was set up as shown in Fig. 1 with an upper span of 150 mm and a lower span of 350 mm. This was selected to create a region of uniform compressive stress in the face sheet with the seeded damage. The load was introduced into the specimen *via* 12 mm diameter steel rollers. A cyclic load was applied using an Instron 8802 servo-hydraulic test machine (fitted with a 100 kN actuator and load cell) over a range of loading frequencies (from 5 to 12 Hz) and amplitudes (from 0.2 to 0.4 kN equating to a bending moment of 20 to 40 Nm in the central region of the specimen). The infrared detector was placed approximately 350 mm from the specimen. A mirror, angled at 45° and placed above the specimen, enabled the top surface to be viewed by the detector and provided a field of view of 120 x 100 mm with a spatial resolution of approximately 0.4 mm per image pixel.

Tests to failure were also conducted with a reduced upper span to increase the bending moment relative to the applied load with the aim to avoid indentation failure at the loading points. Here the detector was arranged to view the side of the specimen to enable the measurement of the change in temperature associated with the heat released at failure. A higher spatial resolution of approximately 0.3 mm per image pixel was used to provide increased detail in the vicinity of the face sheet / core interface.

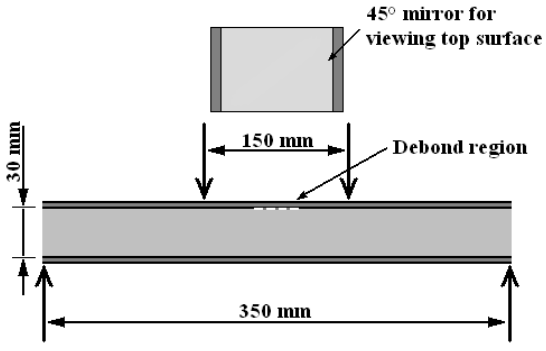

Fig.1 Experimental setup for the four point bend test

The second part of the investigation utilised the DCB test to investigate the stress distribution in the core at the tip of a debonded region. The setup for this is shown schematically in Fig. 2. The total debond length was 50 mm (the hinges were 25 mm long) and located at one end of the beam. The debond was introduced in an identical manner to that adopted for the specimens loaded in four point bending. Specimens of 200 mm length and 32 mm width were cut from panels manufactured from the same material as used in the four point beam bending test. The DCB test was conducted in an Instron E1000 (Electropuls) test machine with a 1 kN actuator and load cell capacity. The hinges were clamped in standard mechanical grips used in tensile testing. The specimen was viewed from the side as in Fig. 2 with the image centred near the crack tip. A spatial resolution of approximately 0.2 mm per image pixel was used for this test.

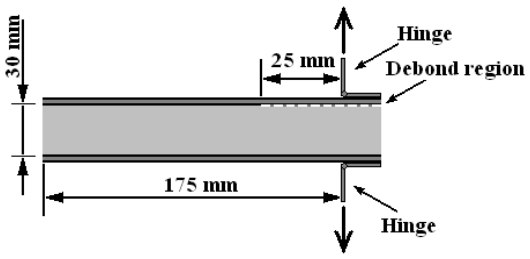

Fig. 2 Experimental setup for the DCB test

A Cedip Silver 480M infrared detector was used to provide the full-field surface temperature *via* a 45° mirror at a frame rate of 383 Hz. The detector is radiometrically calibrated by the manufacturer and therefore able to provide direct temperature readings. The recorded temperature data was then processed using the commercial lock-in thermography software provided by FLIR, to provide the amplitude of the measured temperature (ΔT) at each point in the image [2]. ΔT is obtained relative to a reference signal from the test machine load cell to also provide a phase angle for each measurement point. Data is presented in the non-dimensional form $\Delta T/T$. As the stress in the face sheet in both tests is nominally unidirectional, $\Delta T/T$ is directly proportional to $\Delta\sigma_1$. Therefore the quantity $\Delta T/T$ can be considered as a non-dimensional stress metric that can be used to identify stress concentrations in the face sheet. A 180° phase shift between adjacent data indicates a reversal from tensile to compressive stress or *vice versa*. However, it is known that the foam core is orthotropic [4] and

therefore the thermoelastic response from the foam can only be considered as a qualitative indication of the stress distribution. Further experimental analysis to obtain the thermoelastic constants in each material direction is necessary to obtain a quantitative stress metric.

4 Four point bend test results

TSA data was collected for a range of load amplitudes and debond lengths. Fig. 3 shows the TSA data from the surface of the specimen. The edges of the debond region have been highlighted with dashed lines for clarity. It can be seen that the effect of the debond on the thermoelastic response is barely visible against the noise introduced by the peel ply imprint on the specimen surface resulting from the manufacturing process. To evaluate the redistribution of the stresses across the debond region it was therefore necessary to filter out this noise. This was done by first defining a rectangular area around the debonded region as shown in Fig. 3. Since the stresses across the width of the specimen are nominally uniform it is possible to obtain an average across the specimen width that is representative of the thermoelastic response at a point along the length. Inspection of line plots transverse to the beam confirmed that there is no gradient in $\Delta T/T$ across the width of the specimen. To enable a direct comparison between data obtained at different load levels, the mean value was then normalised against the mean value of $\Delta T/T$ over the complete measurement area, providing the set of normalised curves that are shown in Fig. 4 from a specimen with a 12 mm debond length. The three different loading amplitudes are defined in terms of the imposed bending moment.

It can be seen in Fig. 4 that there is a 4 to 5% decrease in the thermoelastic response across the debonded region. This is due to the shear stress carried by the core being transferred into the face sheet at the debond and adding a local out-of-plane component to the deformation in the face sheet. Therefore a reduction in the compressive stress at the surface of the face sheet occurs and hence a small decrease in the thermoelastic response is observed in this region. Furthermore, the normalised curves coincide almost exactly for all three load amplitudes indicating that the stress redistribution due to the defect is not influenced by the loading level. This would not be the case if there was a load threshold dependent type of behaviour was occurring, such as localised face sheet buckling. A set of fatigue tests at load levels up to twice the highest load amplitude used to obtain the TSA data showed no growth in the debonded region. This result, together with the distinctive load independent decrease in $\Delta T/T$ confirms the non-destructive nature of the tests and the suitability of the technique to locating debond damage within a sandwich structure.

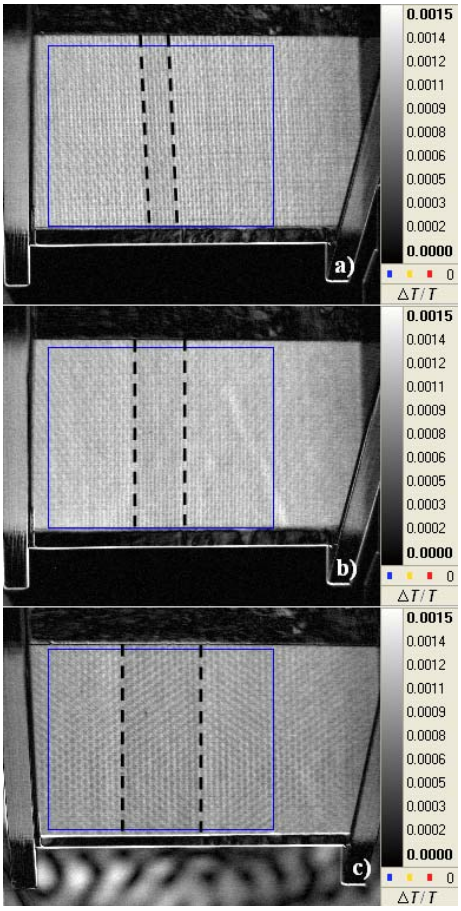

Fig. 3 Non-dimensional TSA data from the compressive face sheet with a) 6 mm, b) 12 mm and c) 18 mm debond lengths

Fig. 5 shows the normalised TSA data from the three debond lengths (6, 12 and 18 mm). A decrease in the thermoelastic response in the debonded region is common to all three debond lengths. However, for the longest debond length (18 mm) the edge of the debond region is marked by a sharp increase in the thermoelastic response. For all three load levels the increase at the edge was observed and can therefore

be related to the aspect ratio (face sheet thickness / debond length) of the damaged region. The indication is that there is an increased compressive stress at the edges of the debonded region and a small additional tensile component within the debond region. The net stress however, remains compressive and hence the debond is not apparent in the phase angle data. The edge effect is observable in the 12 mm debond data as well, but is not significantly greater than the background noise.

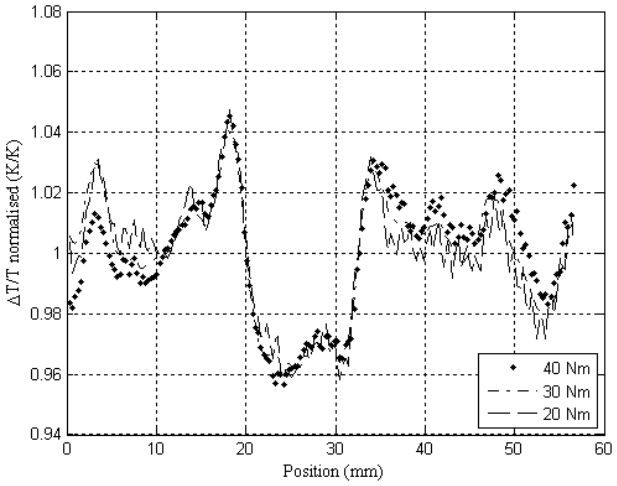

Fig.4 Normalised TSA data from the surface of a beam with a 12 mm debond.

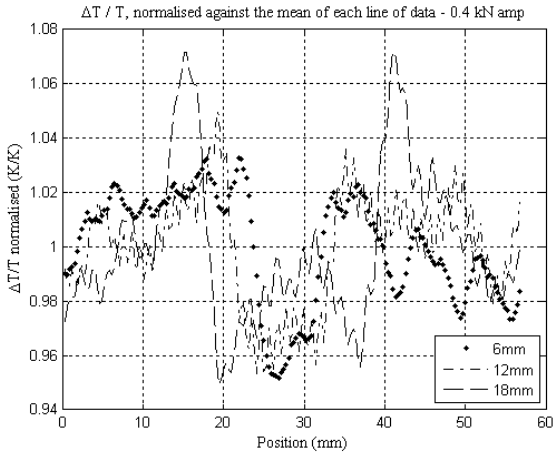

Fig.5 Normalised TSA data from beams with 6, 12 and 18 mm debond lengths.

Thermal data shown in Fig. 6 was also collected from a specimen with an 18 mm debond loaded to failure. Even though the test was conducted in a position control mode, the crack propagated almost instantaneously all the way to the loading points either side of the debond region. To fully capture the failure event, a higher frame rate than the 383 Hz used is required. However, this requires a bespoke calibration process which is subject of ongoing work. Nevertheless, the data acquired is able to give an indication of the heat generated during the formation and propagation of a crack either side of the debond region.

Infrared images of the side of the sandwich beam just before and just after the failure event are shown in Fig. 6. To avoid indentation failure at the loading points, the upper roller spacing has been reduced to 50 mm, and two 20 mm wide pads were placed below each roller to spread the load introduction. In Fig. 6 a) the out-of-plane deformation in the centre of the beam is clearly visible in the infrared image. A small amount of asymmetry can also be identified, as the debond region is slightly closer to the right hand side roller.

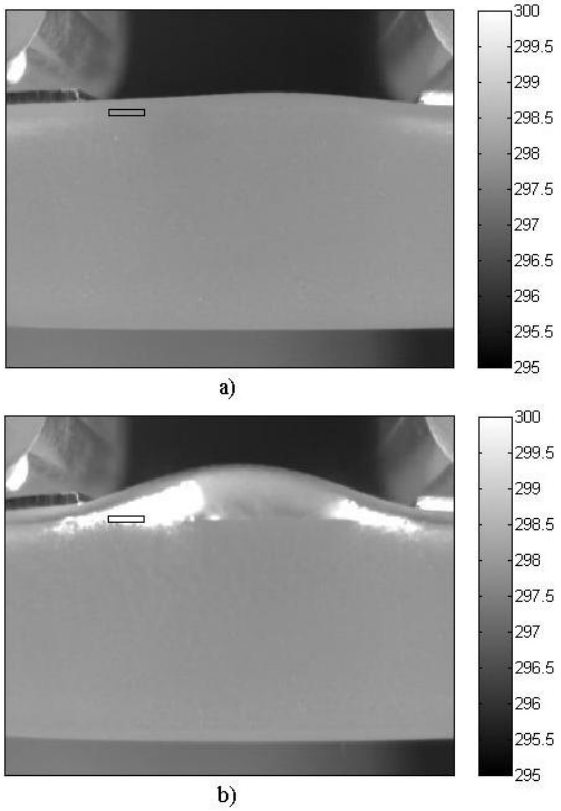

Fig. 6 Thermography images taken at 383 Hz, a) before and b) after failure of the face sheet / core interface adjacent to a seeded debond

Temperature data was collected from the area marked in Fig. 6 at the face sheet / core interface just to the left of the seeded debond, and is presented in Fig. 7 as a function of time. This shows that the heat generated at failure leads to an instantaneous 3 K rise in temperature at the newly formed surface. Knowing the material C_p and averaging over a small volume, the energy released can be computed. The energy associated with the small volume represented by the area in Fig. 6 over a unit width can be calculated as $(\Delta T^*\rho^*C_p^*A)/w$, where A is the area over which the temperature is averaged and w is the width of the specimen. Taking an approximate value of C_p of 900 $Jkg^{-1}K^{-1}$ and a density of 1980 kgm^{-3} [3] for the composite face sheet, yields a value of 1.8 Jmm^{-1} per unit width. This value provides only a first estimate as the errors in material properties used and the spatial calibration and misalignment of the specimen relative to the detector (the temperature measurement is taken from the internal surface and therefore leads to errors in the volume calculation) have not yet been fully evaluated. However, this simple calculation demonstrates how thermography could be used to enable a phenomenological measurement of the crack tip energy release rate, otherwise obtained using kinematic measurements.

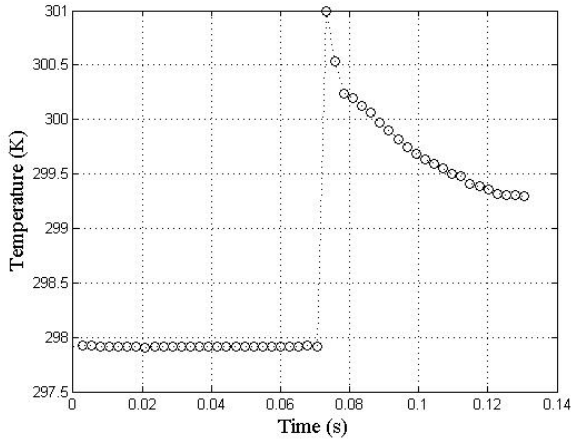

Fig. 7 Temperature of face sheet / core interface against time

5. DCB test results

The DCB test is one many test standards used to obtain interlaminar and face sheet / core interfacial fracture toughness of both laminated composites and sandwich beams. The standard test involves plotting measurements of crack length against load and assessing the area under the resulting curve. The method relies on accurate identification of the crack tip location and hence, the crack length. In the previous section, thermography was used to measure the temperature at the crack tip. In the current section the focus is on measurement of the core stress distribution at a static crack tip associated with crack propagation. However, in line with the discussion in section 4, thermography could be used to assess the energy associated with crack formation and this is the subject of ongoing work.

The data shown in Fig. 8 a) shows the $\Delta T/T$ data at the tip of a crack loaded in a DCB rig in mode I. The speckles in the core region are reflective markers used as tracking points to compensate for the specimen motion in the captured images [3]. The specimen is orientated as *per* Fig. 2 with the crack opening to the right and the region of interest at the crack tip in the upper left quadrant. A localised increase in $\Delta T/T$ identifies the tensile stress in the foam core adjacent to the crack tip. The value obtained within the face sheet is not reliable as the motion in this part of the specimen has not been compensated and hence the measurement of ΔT is spurious in this portion of the image. It is possible to derive the phase of the thermoelastic response relative the applied load. Fig. 8 b) and c) show the corresponding phase and mean temperature data respectively. In the phase image the transition between tensile (-90°) and compressive (90°) regions in the foam core are very clear. The thermography data shows a small amount of heating near the crack tip but this is less than 0.5 K. The data is also presented in Fig. 9 as a line plot, taken along the upper edge of the foam core and passing through the region just below the crack tip, clearly showing the transition in phase.

The work has shown that it is possible to obtain TSA data from the vicinity of the crack-tip, however some refinement is necessary to make the data quantitative and remove the deleterious effects of motion.

6 Conclusions

It has been shown that TSA can be used to assess subsurface damage in sandwich structures by studying the stress field at the surface. The severity of the damage manifests itself in terms of the profile of the TSA data across the damaged region.

Differences in the shape of the curve can be directly related to the severity of the damage and hence correlated to the remnant strength of the sandwich structure. Thereby a methodology has been established by which TSA can be used as a non-destructive evaluation tool for assessing damage in sandwich structures.

Furthermore, initial measurements have shown that TSA can be used to assess the crack tip stress fields in foam cored sandwich structures as well as provide an alternative means of assessing interfacial fracture toughness.

References

[1] R.J.H. Paynter and A.G. Dutton "The use of a second harmonic correlation to detect damage in composite structures using thermoelastic stress measurements". *Strain*, Vol. 39, pp 73-78, 2003

[2] J.M. Dulieu-Barton and P. Stanley "Development and applications of thermoelastic stress analysis". *Journal of Strain Analysis*, Vol. 33, No. 2, pp 93-104, 1998

[3] R.K. Fruehmann, J.M. Dulieu-Barton and S. Quinn "On the thermoelastic response of woven composite materials". *Journal of Strain Analysis*, Vol. 43, pp 435-450, 2008

[4] S. Zhang, J.M. Dulieu-Barton, R.K. Fruehmann, and O.T. Thomsen, "A methodology for obtaining material properties of polymeric foam at elevated temperatures", *Experimental Mechanics*, in press.

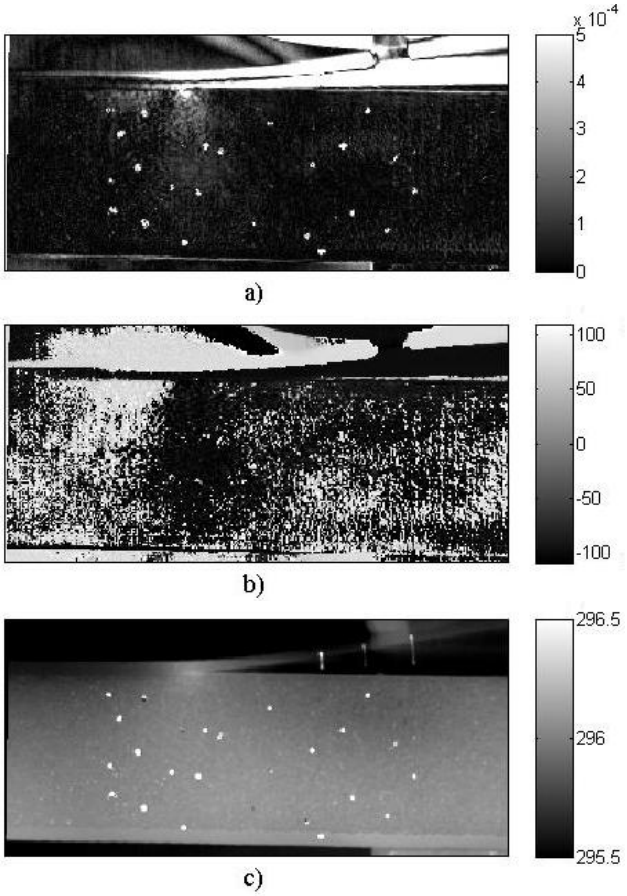

Fig. 8 a) $\Delta T/T$ data from the specimen side, b) corresponding phase image and c) mean temperature

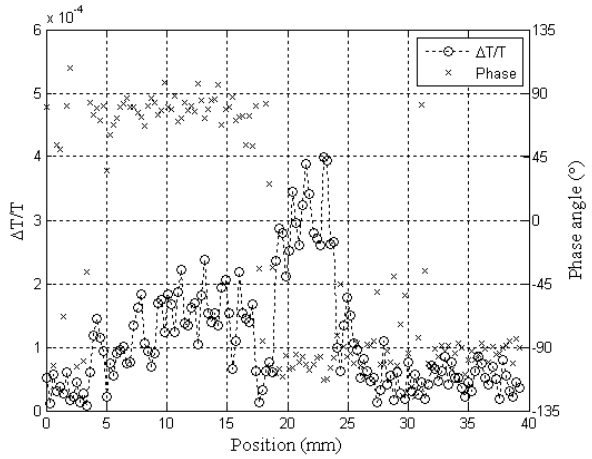

Fig. 9 Line plots of $\Delta T/T$ and phase angle from within the foam adjacent to the face sheet